



Estimating Groundwater Inflow to The Underground Mine Works using a 3D Groundwater Model at Vein Kubang Cicau, UBPE Pongkor

KORY YOHANA ADINDA NAIBORHU^{1,2}, KOMANG ANGGAYANA¹, LILIK EKO WIDODO¹,
and ARYO PRAWOTO WIBOWO¹

¹Mining Engineering, Faculty of Mining and Petroleum Engineering, Institut Teknologi Bandung
Jln. Ganesha 10, Bandung, 40132, Indonesia

²Inspektorat Jenderal, Ministry of Mineral Resource and Energy, South Jakarta, Indonesia

Corresponding author: kory.yohana@esdm.go.id

Manuscript received: May, 31, 2023; revised: April, 17, 2024;

approved: September, November, 01, 2024; available online: December, 7, 2024

Abstract - Estimating groundwater inflow to underground mines is essential for ensuring that mining activities can be conducted safely and continuously. Research conducted at UBPE Pongkor indicates that the veins have the fault connectivity with the Kubang Cicau vein showing potential for deeper mining, while other veins are expected to become exhausted. As the result, the Kubang Cicau vein will likely be at a lower elevation in the future. Planning decisions regarding groundwater control measures, such as dewatering, can be made in advance, contributing to a more efficient assessment of the economic feasibility of mining development. Groundwater modeling using MODFLOW software predicted a maximum groundwater discharge of 55 L/s. To address the model uncertainty, a sensitivity analysis was performed by increasing the hydraulic conductivity parameter by two order of magnitude, as this value significantly affects groundwater inflow. Conversely, decreasing the hydraulic conductivity by two order resulted in a new discharge estimate of 87 L/s. In the worst-case scenario, with the highest specific storage values, the inflow increased to 76 L/s. This demonstrates that although changes in specific storage have a notable effect on groundwater inflows, the impact is less pronounced compared to the changes in hydraulic conductivity. Nonetheless, Ss remains a key parameter, particularly in transient simulations where storage plays a more significant role in the system response to changes in water levels.

Keywords: vein, groundwater inflow, sensitivity analysis, Kubang Cicau

© IJOG - 2024

How to cite this article:

Naiborhu, K.Y.A., Anggayana, K., Widodo, L.E., and Wibowo, A.P., 2024. Estimating Groundwater Inflow to The Underground Mine Works using a 3D Groundwater Model at Vein Kubang Cicau, UBPE Pongkor. *Indonesian Journal on Geoscience*, 11 (3), p.423-435. DOI: [10.17014/ijog.11.3.423-435](https://doi.org/10.17014/ijog.11.3.423-435)

INTRODUCTION

The Unit Bisnis Pertambangan Emas (UBPE) Pongkor, plans to develop its mining level deeper, particularly in the Kubang Cicau vein. This prospect area will eventually have the lowest elevation compared to other vein prospect areas. Groundwater inflows into underground mines can pose significant challenges, both practically and economically. Unexpected inflows can lead

to poor working conditions, reduced safety standards, and costly delays in excavation and operations. Therefore, having a reliable estimate of mine inflow is crucial. By planning groundwater control measures, such as dewatering, in advance, the mine can conduct a more efficient assessment of the economic feasibility of its development. The aquifers within the researched area consist of fractured zones. Groundwater flow in this location is not primarily controlled by lithology,

but is significantly influenced by structural features such as veins, faults, and fractured media (Milesi *et al.*, 1999). Previous investigations have demonstrated connectivity between the fault zone and the mined vein zone, with the fault zone predicted to act as a continuous, orthogonal high-permeability zone aligned with the vein direction (LAPI ITB, 2021). A conceptual model of the hydrogeological and groundwater systems is used to develop a numerical model, which serves as a predictive tool for estimating groundwater discharge entering the mine site (LAPI ITB, 2021).

Location of the Mine Site

The Antam UBPE Pongkor is located in the Bogor Regency of West Java Province, approximately 50 km south of Jakarta (Figure 1). This underground mine is actively operated by P.T. Antam and consists of four mining blocks: Ciurug Mine, Ciguha Mine, Kubang Cicau Mine, and Gudang Handak Mine.

According to the LAPI ITB report (2021), the area has a monsoon tropical climate characterized by high humidity, averaging over 85 %. It experiences very wet conditions, with most months classified as wet one and an average rainfall exceeding 200 mm per month. The an-

nual average temperature is 25.5°C, ranging from approximately 24 to 27°C. The total annual average rainfall is around 3,461 mm, with the lowest in June (about 160 mm) and the highest value in November (approximately 360 mm).

Geological Setting

Epithermal mineralization deposits associated with volcanism in the western part of Java, including those in Pongkor, are found on the edges and within the Bayah Dome (Milesi *et al.*, 1999). This geological unit spans an area of approximately 40 × 80 km and consists of calc-alkaline rocks ranging from rhyolitic to andesitic, dating from the Oligocene to Quaternary period, with several layers of Miocene-aged limestone and sandstone (Milesi *et al.*, 1999).

The Pongkor area and its surrounding regions are composed of volcanic rocks such as tuff, tuff breccia, andesite breccia, and lava (Figure 2), which are categorized into three volcanic units: the Upper Volcanic Unit, Central Volcanic Unit, and Lower Volcanic Unit (P.T. Antam UBPE Pongkor, 2020). The Upper Volcanic Unit features Pliocene-aged andesite lava and breccia, while the Central Volcanic Unit includes lapilli, tuff breccia, tuff, and epiclastic silt, intruded by a rhyolitic dome. The Lower Volcanic Unit is

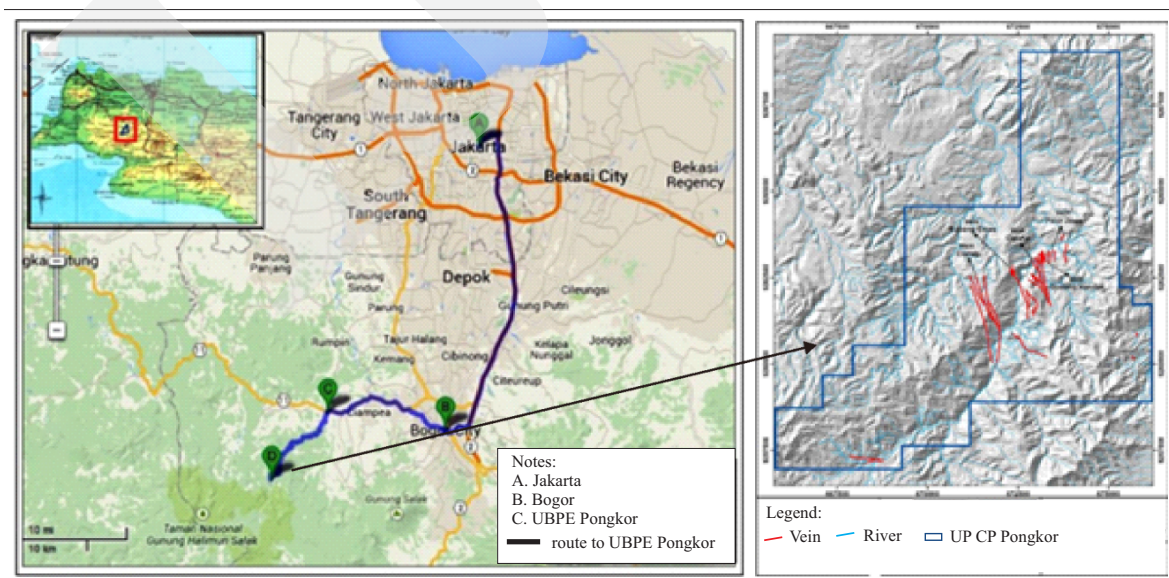


Figure 1. Access to Antam UBPE Pongkor (modified from P.T. Antam UBPE Pongkor, 2020).

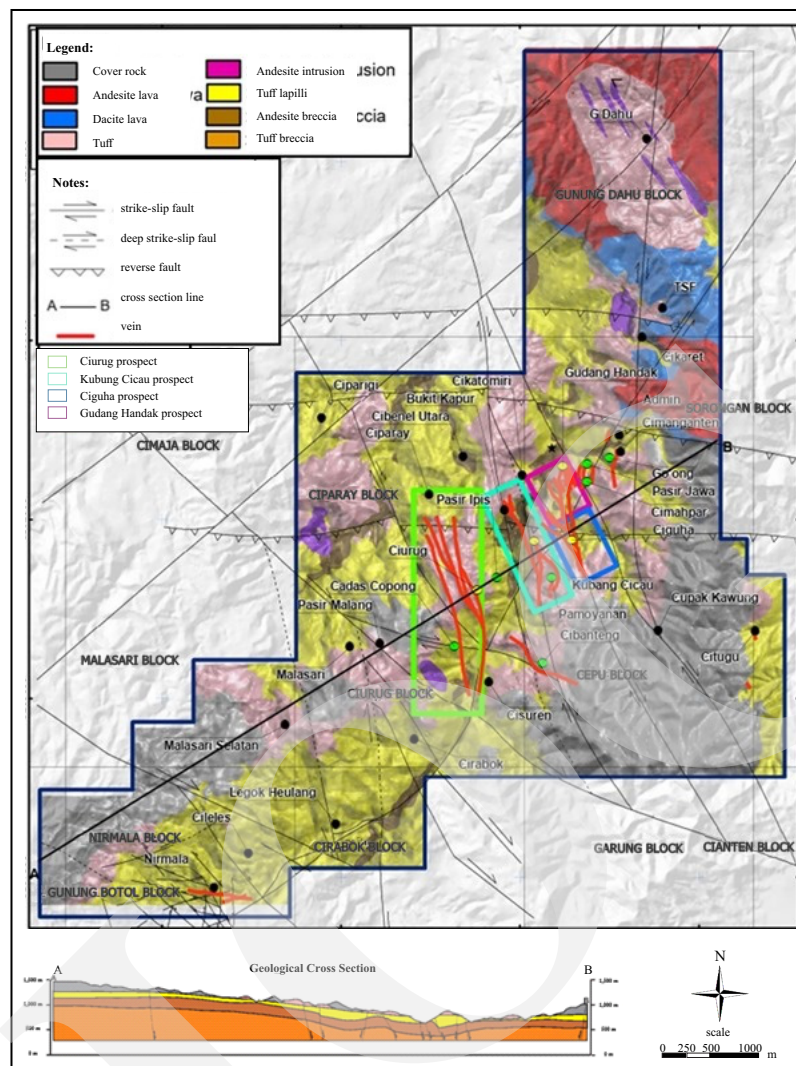


Figure 2. Geological map of Mount Pongkor area (modified from P.T. Antam UBPE Pongkor, 2020).

characterized by subaqueous graded bedding and consisting of andesitic lava, altered andesitic breccias, and tuff breccias (P.T. Antam UBPE Pongkor, 2020).

In the Pongkor area, three main structural directions are observed: the oldest is NE-SW (northeast-southwest), followed by NW-SE (northwest-southeast), and finally normal faults (descending) (Figure 1). The NE-SW and NW-SE directions represent conjugate strike-slip faults resulting from the Pliocene-aged Javanese subduction, which led to the formation of a caldera in the middle of the Pongkor Prospect. This caldera structure reactivated the conjugate faults, transforming them into tension structures (P.T. Antam UBPE Pongkor, 2020).

The mineralization in the Mount Pongkor area is primarily classified as a low epithermal sulfide mineralization, characterized by quartz veins containing gold (gold-bearing quartz veins). Within the Pongkor Mineralization Complex, several quartz veins run relatively parallel to each other. The four main veins are as follows:

1. Ciurug vein (CU): approximately 1.5 km in length, trending NW-SE, about 4-6 m wide, with a slope of approximately $\pm 60^\circ$ towards the northeast.
2. Kubang Cicau vein (KC): approximately 1.2 km long, also trending NW-SE, about 4-5 m wide, with a slope of approximately $\pm 0^\circ$ towards the northeast.

3. Ciguha vein (CG): approximately 1.4 km in length, trending NW-SE, about 4-5 m wide, with a slope of approximately $\pm 80^\circ$ towards the northeast.
4. Gudang Handak vein (GH): approximately 0.8 km long, trending NW-SE, about 3-4 m wide, with a slope of approximately $\pm 80^\circ$ towards the northeast.

Hydrogeological Conditions

The groundwater flow at the case site is primarily influenced by fracturing and geological structures. According to the interpretation by Milesi *et al.* (1999), the veins found in Pongkor are affected by the presence of aquifers or surface water. This is evidenced by the development of vein fields, which are heavily oxidized, leading to the formation of manganese oxidation zones. In the field, fracturing that releases water is often marked by the presence of Mn-oxide.

Aquifer zones are predicted to exist in rock masses with intensive fracturing, particularly in vein zones and fault structures. The fracturing process, driven by dissolution and erosion, enlarges these fractures to form open cavities, especially in the vein zones. Additionally, aquifer connectivity is likely influenced by fault structures. In the studied area, the fault zones are expected to be significant flow zones. These zones typically include a fault core (FC) surrounded by a damaged zone (DZ). The fault core, which experiences the most intense strain, is generally located at the center of the fault zone and accommodates most of the displacement. The damaged zone, characterized by secondary structures such as fractures and minor faults extending into the footwall and hanging wall, accommodates the remaining strain (Bense *et al.*, 2013).

A permeability model for the fault zone in the studied area suggests that a higher permeability is found in the damaged zone due to increased fracturing (Bense *et al.*, 2013). Given these conditions, groundwater flow in the studied area is likely anisotropic and non-uniform due to the complexity of the hydrogeological system.

The groundwater is also predicted to have direct connectivity with surface water, particularly in areas where rivers intersect the fracturing system, as well as from shallow groundwater systems intersecting these fractures. A chemical and stable isotope analysis of water (^{18}O and ^2H) conducted by LAPI ITB in 2021 had concluded that the Cikaniki River was contributed into the inflow of groundwater observed in the UBPE Pongkor Underground Mine (Figure 3).

Historical Groundwater Inflow

P.T. Antam UBPE Pongkor has recorded groundwater inflow in each mining block by measuring the inflow at collection drain locations. The collection drain is a channel designed to collect groundwater seepage from all underground faces. Antam recorded the data from 2018 to 2020, although some data points are incomplete or discontinuous. A statistical summary of groundwater inflow discharge at each Pongkor mining block location is provided in Table 1.

METHODS AND MATERIALS

Conceptual Model

Permeability or hydraulic conductivity, in fractured rocks is more complex than in porous sedimentary rocks (Zhou, 2022). In fractured rocks, geological structures play a major role in shaping hydrogeological systems and controlling groundwater flow patterns. A limited number of hydraulic conductivity field tests may not provide an adequate estimate of the spatial distribution of hydraulic conductivity across a rock mass. Therefore, empirical methods that assess hydraulic conductivity and rock mass connectivity are often used (Cahyadi *et al.*, 2015). These methods estimate spatial distribution by analyzing correlations between field-measured hydraulic conductivity (K) and various geotechnical properties within the test zone or section.

The empirical HC model may provide a useful tool to predict hydraulic conductivity of fractured rocks based on measured HC-values (Ku *et al.*,

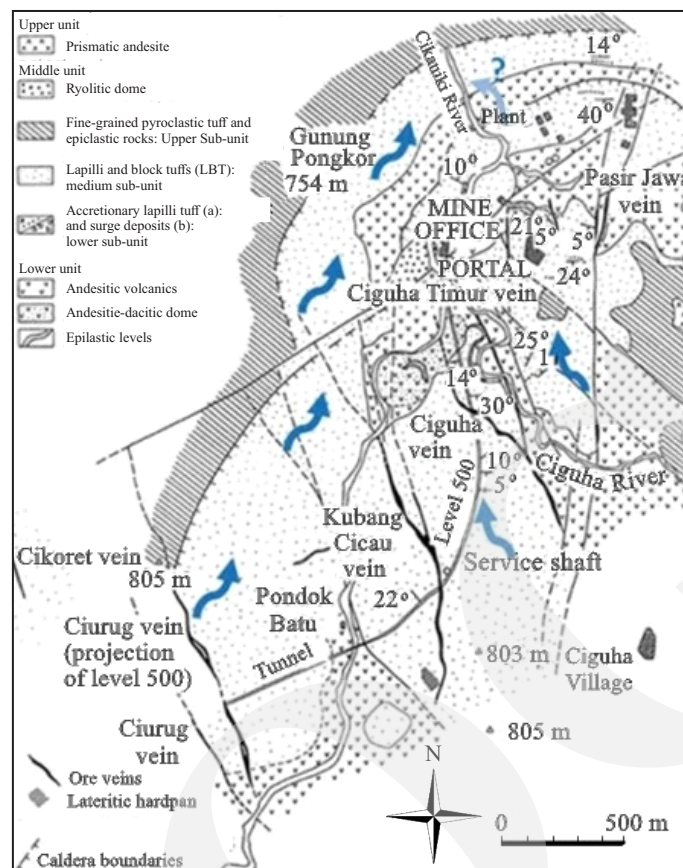


Figure 3. General patterns of groundwater flow (modified from Milesi *et al.*, 1999).

Table 1. Resume of Historical Data Statistics of Groundwater Inflow at Pongkor

Parameter	Ciurug A (L/s)	Ciurug B (L/s)	Ciurug C (L/s)	Kubang Cicau(L/s)	Ciguha (L/s)	Gudang Handak (L/s)
Number of data	106	94	63	6	14	47
Mean	33.0	141.2	33.2	21.8	16.0	77.8
Median	33.3	144.0	34.0	21.8	16.7	80.0
Mode	39.0	151.0	35.0	24.8	13.3	31.0
Standard Deviation	9.5	27.5	7.0	9.8	2.7	36.5
Sample Variance	5.3	45.2	3.0	5.8	0.5	79.7
Minimum	9.5	47.0	19.8	8.2	13.3	24.0
Maximum	58.0	191.8	49.0	37.3	20.0	154.5

2009). The objective function (Iskandar *et al.*, 2014) can be expressed as follows:

$$HC = \left(1 - \frac{RQD}{100}\right) \cdot (DI) \cdot (1 - GCD) \cdot (LPI) \dots\dots (1)$$

where:

- RQD is Rock Quality Designation (a measure of rock fracture, ranging from 0 to 100).
- DI is Degree of Interconnection (a factor that represents how interconnected the fractures or porous networks are in the rock mass).

- GCD is Groundwater Conductivity Decay (a factor that accounts for the decrease in groundwater conductivity over distance or time).
- LPI is Lithology Permeability Index (an index reflecting the permeability characteristics of the lithology in question).

Hydraulic Properties

Hydraulic conductivity tests at the studied site were derived from previous studies, including nineteen packer test intervals on the GH-GT01 boreholes (located in Gudang Handak

vein) and two pumping tests on the KCD 36 (located in Kubang Cicau vein; Figure 4) and GH-GT-01A (located in Gudang Handak vein; Figure 5) boreholes (P.T. Antam UBPE Pongkor, 2020). Table 2 presents a summary of hydraulic conductivity values by depth, based on the packer tests conducted on the GH-GT-01 borehole. Table 3 provides the hydraulic conductivity values from the pumping test results.

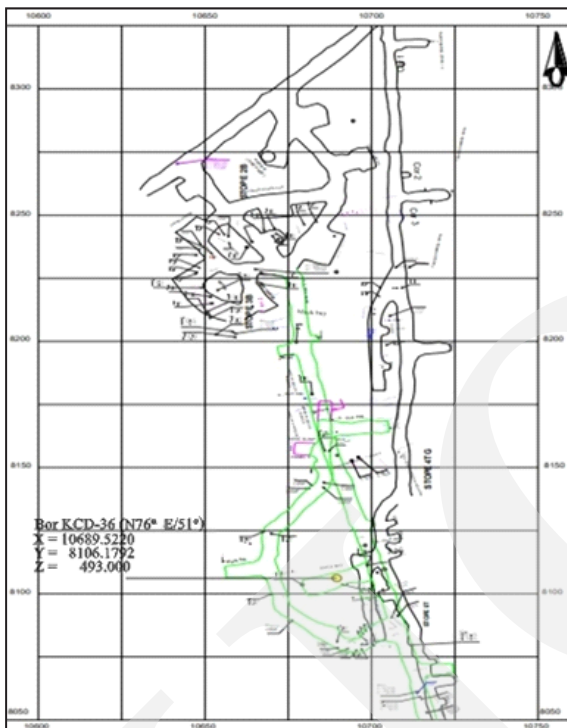


Figure 4. Pumping test location on KCD-36, Kubang Cicau vein (P.T. Antam UBPE Pongkor, 2020).

The side rocks, identified as andesite breccia or tuff breccia, have an average hydraulic conductivity value of 3.5×10^{-7} m/s. In contrast, the vein zone exhibits a higher average conductivity value of 1.6×10^{-5} m/s. The pumping test results indicate a hydraulic conductivity of 1.29×10^{-5} m/s, with a specific storage value of 1.1×10^{-4} (without unit).

Groundwater Model Tools

One of the key challenges in simulating groundwater flow is the development of a robust conceptual model that accurately represents fault

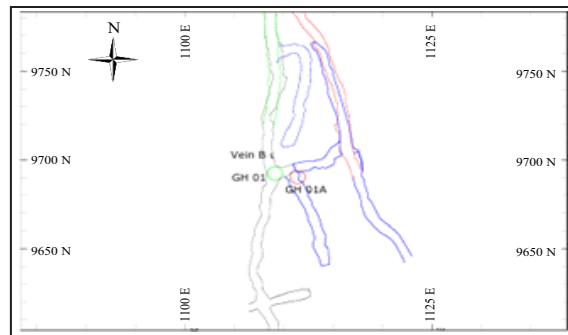


Figure 5. Pumping test location on GH-GT-01A and packer test on GH-GT01, Gudang Handak vein (P.T. Antam UBPE Pongkor, 2020).

and fracture aquifers. To construct such a model, site-specific and hydraulic data must be gathered and analyzed to improve understanding and modeling of the groundwater system. The level of conceptual model in detail depends on the purpose and resolution of the groundwater simulation. Recently, several software platforms have been developed with user-friendly graphical interfaces (GUIs), providing implicit modeling tools that facilitate the creation of conceptual models and their conversion to numerical solutions.

Groundwater flow models typically solve problems using one of three algorithms: finite-difference (FD), finite-element (FE), or finite-volume (FV) methods. In this study, the groundwater model was developed using MODFLOW, a widely used tool for constructing three-dimensional (3D) numerical groundwater flow models based on the finite-difference method. Developed by the U.S. Geological Survey (USGS), MODFLOW can simulate both steady-state and transient groundwater flow in one, two, or three dimensions.

Although fracture networks in fractured or weathered aquifer systems introduce discontinuities and anisotropies, these effects can be minimized at larger scales using an equivalent porous medium (EPM) approach (Surinaidu *et al.*, 2014). Therefore, the groundwater flow in the studied area was simulated using the EPM approach within the MODFLOW framework.

Model Domain and Discretization

The model domain was extended beyond the mine site to accommodate boundary conditions.

Table 2. Resume of Hydraulic Conductivity Value (K) Packer Test Results in GH-GT01

Depth From (m)	Depth To (m)	K (cm/s)	K (m/s)	Lithology	RQD**
3	8	3.35×10^{-5}	3.35×10^{-7}	Andesite breccia	78
8	13	3.74×10^{-5}	3.74×10^{-7}	Andesite breccia	73.2
13	18	1.19×10^{-4}	1.19×10^{-6}	Tuff breccia	74.2
18	23	2.91×10^{-4}	2.91×10^{-6}	Tuff breccia	74.8
23	28	3.51×10^{-4}	3.51×10^{-6}	Tuff breccia + Andesite + Vein	76
28	33	1.71×10^{-3}	1.71×10^{-5}	Andesite + Vein	62.6
38	43	1.71×10^{-3}	1.71×10^{-5}	Andesite + Vein	57.4
43	48	1.71×10^{-3}	1.71×10^{-5}	Andesite + Vein	47.6
48	53	1.71×10^{-3}	1.71×10^{-5}	Andesite + Vein	22.6
53	58	1.71×10^{-3}	1.71×10^{-5}	Andesite breccia + Vein	27.2
58	63	1.39×10^{-3}	1.39×10^{-5}	Andesite breccia + Vein	21.4
63	68	1.18×10^{-3}	1.18×10^{-5}	Andesite breccia + Vein	34.6
68	73	2.35×10^{-5}	2.35×10^{-7}	Tuff breccia	33.8
73	78	2.26×10^{-5}	2.26×10^{-7}	Tuff breccia	28.2
78	83	2.19×10^{-5}	2.19×10^{-7}	Tuff breccia	24.8
83	88	1.83×10^{-5}	1.83×10^{-7}	Tuff	29.2
88	93	5.38×10^{-5}	5.38×10^{-7}	Tuff	30.2
93	98	5.43×10^{-5}	5.43×10^{-7}	Tuff	54.4
98	103	5.40×10^{-5}	5.40×10^{-7}	Tuff	36.6
Average K			6.42×10^{-6} m/s		

Table 3. Resume Hydraulic Conductivity Value of Pumping Test Results on KCD 36 and GH-GT-01A

Hole ID	Interval Screen (m depth)	K (m/s)	Ss (m ⁻¹)	Method
KCD 36	22.3–30.3	2.27×10^{-5}	1.05×10^{-4}	Barker, 1988
	38.3–42.3			
	46.3–58.3			
	78.3–106.3			
GH-GT-01A	3.0–105.0	3.15×10^{-6}	1.15×10^{-4}	Barker, 1988

A grid size of 10x10x10 m was used in the model, and the grid was arranged according to the mine design. The dimensions of the model boundaries and the grid sizes are details in Table 4 and illustrated in Figure 6. Additionally, the model-grid elements were discretized to represent major geological structures, such as faults, as well as key features of the historical mines and mine plans, including shafts and drifts.

Model Parameters and Boundary Conditions

Numerical simulations were performed using the finite difference method (FDM) with MODFLOW, applying the hydraulic parameters listed in Table 5. The main river recharging the Ciurug and Kubang Cicau aquifer systems is the Cikaniki River. The Cikaniki River and its tributaries serve as the primary surface boundary condition (river boundary), having a hydraulic connection with the groundwater system formed by the mining excavations. This system is modeled as a drain boundary, with drain values estimated from measured discharge data. At a certain depth, below 200 m asl., it is assumed that there is no groundwater flow, establishing a no-flow boundary condition, as illustrated in Figure 7. Other river parameters that build the model are river stage (elevation along streamline following

Table 4. Resume Model Boundaries and Model Dimensions

Model Dimension		Distance	Grid Size	Grid Sum	Total Block
Easting (column)	Min	9100	2500	10	250
	Max	11600			
Northing (row)	Min	7200	2800	10	280
	Max	10000			
Elevation	Min	200	800	10	80
	Max	1000			

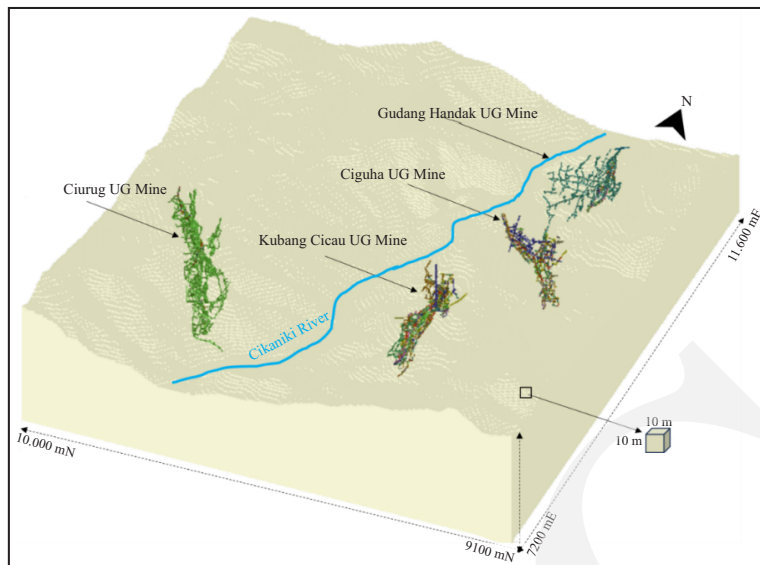


Figure 6. Three-dimensional domain model of groundwater grid model.

Table 5. Hydraulic Parameter

Parameter	Value	Remarks
Hydraulic Conductivity (K)	Based on hydraulic conductivity distribution model (Figure 6)	Average K in model= 2.12×10^{-7} m/s (based on HC System)
Specific Storage (Ss)	$Ss = 1.05 \times 10^{-4}$	Calculated based on single well pumping test from KCD
Recharge (R)	1,260 mm/year	30 % from average precipitation, NRECA calculations (Antam, 2020)
Initial Head	Model calibration (steady state)	

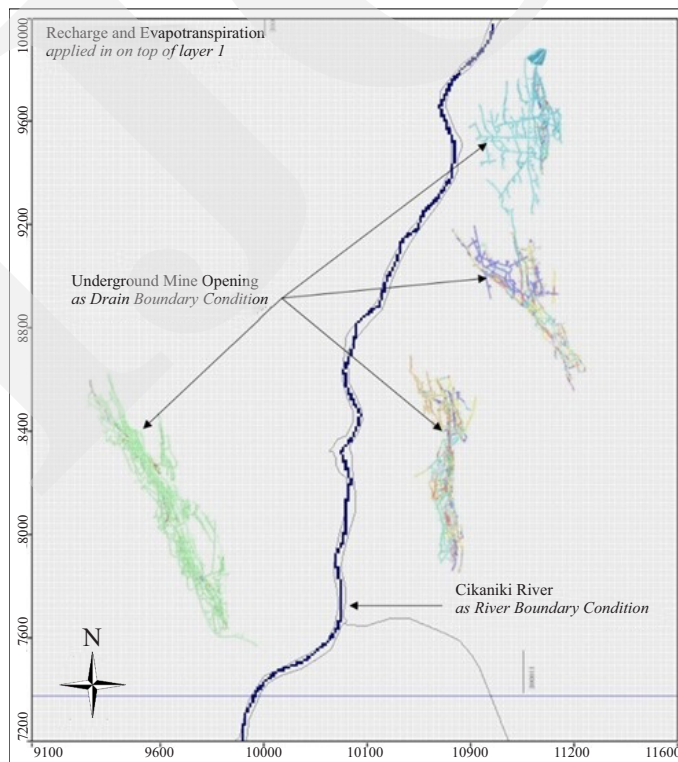


Figure 7. Cikaniki River as a boundary condition.

topography), river bottom 2 m deep relative to river stage, riverbed thickness 0.5 m, riverbed 1.00 E-04 m/s, and river width 5 m. Recharge from Cikaniki River provided for the model is as in Figure 8.

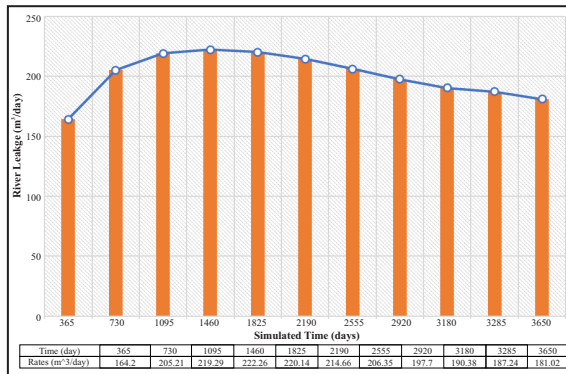


Figure 8. Recharge from Cikaniki River provided for the model.

RESULT AND DISCUSSION

HC System Result

Based on the results of HC calculations, the correlation equation for hydraulic conductivity and HC is obtained as follows:

$$K = 0.0018 (HC^{1.5116}) \dots\dots\dots (2)$$

Based on this HC equation, a distribution model and statistical analysis for the K value can be obtained as shown in Figure 9 and Table 6.

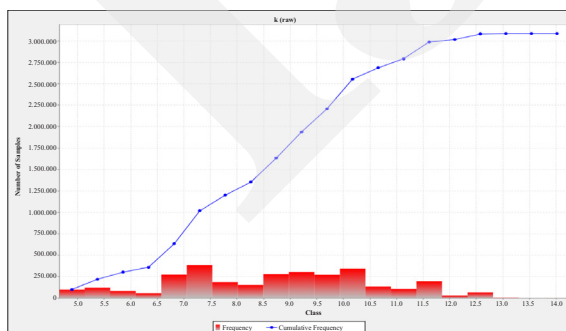


Figure 9. Hydraulic conductivity distribution model based on HC equation, in the studied area.

The cross-plot showing the empirical relationship between the Hydraulic Conductivity

Table 6. Resume of Hydraulic Conductivity

Parameter	- Log K	K (m/s)
Mean	6.673801	2.12×10^{-7}
Minimum value	4.655145	2.21×10^{-5}
Maximum value	12.2538	5.57×10^{-13}
Median	8.917697	1.21×10^{-9}
Variance	3.532463	2.93×10^{-4}
Standard Deviation	1.879485	1.32×10^{-2}
Coefficient of variation	0.216685	6.07×10^{-1}
Skewness	-0.06471	1.16
Kurtosis	2.254418	5.57×10^{-3}

The average K value, 2.12×10^{-7} m/s, will then be used to build a groundwater model.

(K) and the HC parameter using the equation $K = 0.0018 (HC^{1.5116})$ (Figure 10). The red line represents the fitted model, and the calculated R-square value is 0.99, indicating a very strong correlation between those two variables. This strong R-square suggests that the empirical equation provides a reliable estimate of hydraulic conductivity based on the HC parameter.

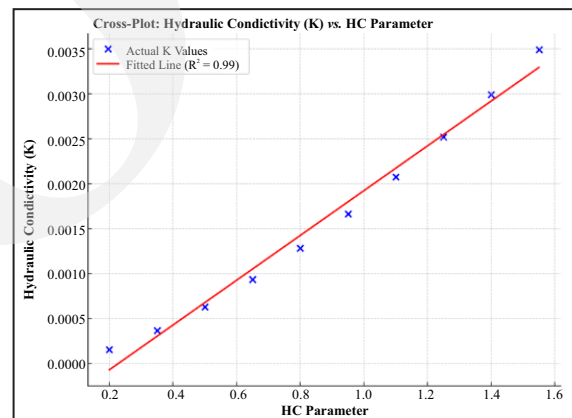


Figure 10. Cross-Plot Hydraulic Conductivity vs HC Parameter.

Model Transient Calibration

The model was calibrated using transient simulations. The calibration period lasted 70 hours (or three days), aligning with the pump test conducted at the Kubang Cicau Mine from December 9th to December 12th, 2014. The model was designed to calibrate head changes by comparing model results with actual conditions over time. In Figure 11, the red squares represent observed data, while the blue line shows the interpolated values.

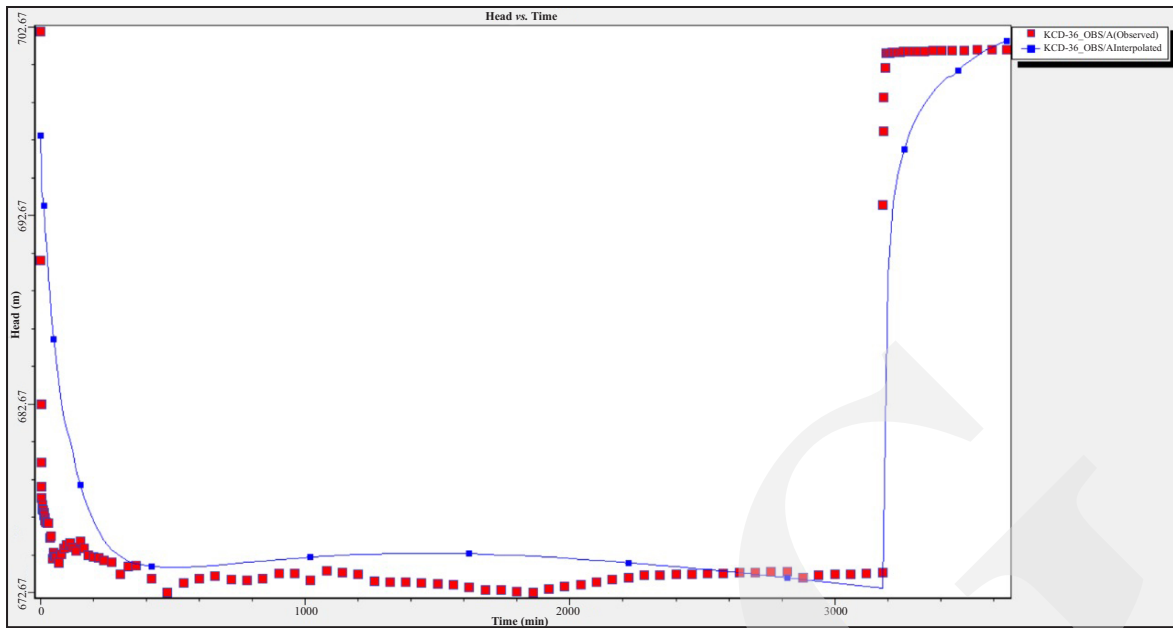


Figure 11. Model calibration results of pumping test on KCD 36.

A regression analysis comparing the model simulation results with actual discharge observations is shown in Figure 12. The analysis demonstrates a strong correlation between the model and observed data. The regression analysis conducted during model calibration further supports the accuracy of the predictions, with a strong correlation ($r^2 = 0.8612$) between observed discharge data and simulated results. This high degree of fit indicates that the model can be reliably used for future predictions of groundwater inflows.

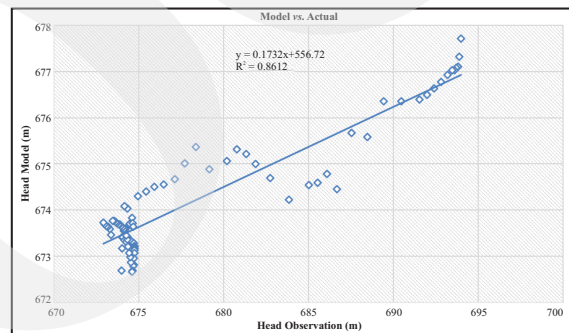


Figure 12. Graph of change head model results vs. observation results from pumping test on KCD-36.

Model Prediction

The prediction of the groundwater inflow model on mine progress was carried out using the Next Development/Production assumptions as follows:

- Level 470 m asl. to 460 m asl. → year 2022
- Level 460 m asl. to 450 m asl. → year 2023
- Level 450 m asl. to 440 m asl. → year 2024
- Level 450 m asl. to 440 m asl. → year 2025
- Level 440 m asl. to 430 m asl. → year 2026
- Level 430 m asl. to 420 m asl. → year 2027

Based on the assumptions used, the groundwater inflow was obtained as shown in Table 7, where

the model results predict progress to level 420 m asl. ranging from 38 to 55 L/s.

Cross-validation of the simulation results could ideally be performed using data from pumping activities in 2022 and 2023. However, such validation was not possible due to the lack of measurement data and/or the absence of pumping activities during that period.

Sensitivity Analysis

Sensitivity analysis is an effective tool for analysing the responses of some selected performance measure of a groundwater flow problem to perturbations of the parameters

Table 7. Groundwater Inflow Rates

Year	Time (day)	Model Results	
		Rates (m ³ /day)	Rates (L/s)
2022	1460	3332.6	38.57
2023	1825	3752.5	43.43
2024	2190	3859.4	44.66
2025	2555	4165.8	48.21
2026	2920	4320.2	50.00
2027	3180	4749.6	54.97

(Yung, 1990). In this analysis, hydraulic conductivity and specific storage was chosen as the parameter of interest. Several studies (Foster and Maxwell, 2018; Castro and Goblet, 2003; Sameh *et al.*, 2020; Zhang *et al.*, 2022) conclude that conductivity plays a significant role in influencing water discharge. Specific storage is a hydrogeological parameter that must be given more attention and, if estimated in situ at an appropriate scale, could improve understanding of groundwater storage and increase confidence in the modelling of groundwater systems (Chowdhury *et al.*, 2022).

The hydraulic conductivity (K) values in Table 6 show a significant range, with a minimum K of 10^{-13} m/s and a maximum of 10^{-5} m/s, spanning eight orders of magnitude. The standard deviation of approximately 10^{-2} m/s reflects a large variability in the data, indicating that K is highly variable across the site. To fully capture the potential uncertainties or variations in the system, sensitivity analysis involved adjusting the hydraulic conductivity and specific storage parameters by two order of higher and lower magnitude across each grid defined in the model.

The sensitivity analysis results indicate that under normal scenarios, the maximum groundwater inflow is 54.97 L/s. In the worst-case scenario (increased by two orders), the highest hydraulic conductivity value, the inflow significantly increases to 103 L/s and the highest specific storage value, the inflow rises to 91 L/s as illustrated in Figure 13. This shows that while changes in specific storage have a significant effect on groundwater inflow, the impact is less pronounced compared to changes in hydraulic conductivity. Nevertheless, specific storage remains a key parameter, especially in transient simulations where storage plays a more significant role in the system's response to changes in water levels.

When comparing the model results with historical data, it was noted that the maximum inflow recorded at Kubang Cicau was 37 L/s, which is considerably lower than the model predictions under both normal and worst-case scenarios. This case suggests that the model is conservative, likely accounting for future deepening of the mine and increased hydraulic connectivity, which will lead to greater inflows over time.

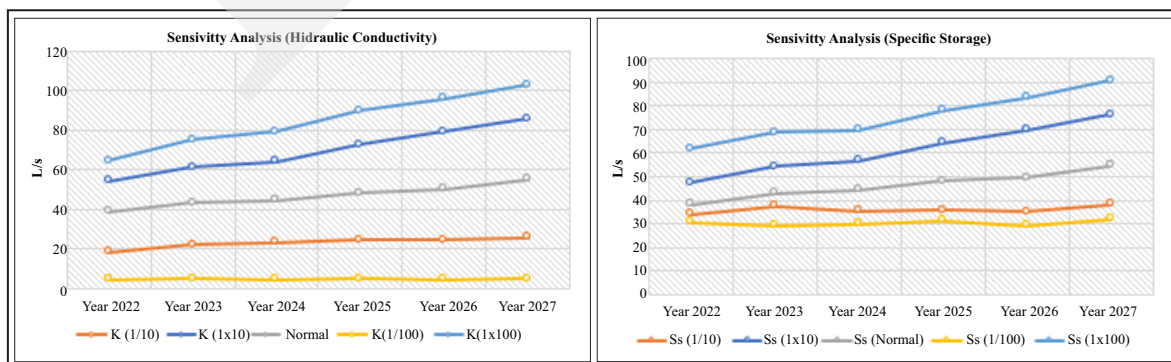


Figure 13. Sensitivity analysis to hydraulic conductivity and specific storage.

The projected inflows from the model, particularly the rising trend from 39 L/s in 2022 to 55 L/s by 2027, indicate that the mine will experience gradually increasing groundwater inflow. This is in line with the expectation that deeper mine openings will intersect more permeable geological structures, such as fault zones and fracture networks, leading to higher inflows. As the result, the model suggests that current dewatering systems may need to be upgraded to handle these future inflows effectively.

CONCLUSIONS

The statement accurately describes the groundwater modeling and sensitivity analysis conducted for the Kubang Cicau vein at Pongkor Mine. The use of MODFLOW, a three-dimensional finite-difference method, is consistent with standard practices in hydrogeological modeling. The importance of hydraulic conductivity (K) and specific storage (Ss) in groundwater flow simulations is well-established.

The conclusion that hydraulic conductivity has a more significant influence on groundwater inflows compared to specific storage aligns with general hydrogeological principles. This finding is supported by research showing that variations in hydraulic conductivity can dramatically affect inflow rates in mining environments.

The emphasis on careful calibration and validation of groundwater models, particularly for mine dewatering management, is crucial. This approach helps in optimizing dewatering strategies and managing water inflow risks effectively.

However, the statement about the Cikaniki River's interaction with the groundwater system being influent is not directly supported by the given search results. The search results do mention the Cikaniki River in relation to a mining area, but they do not explicitly confirm an influent relationship.

Additionally, while the search results discuss groundwater inflow increasing with mining depth in some cases, they also indicate that in other sce-

narios, deeper mines may experience decreased inflow rates. This suggests that the relationship between mining depth and groundwater inflow can vary depending on specific geological and hydrogeological conditions.

ACKNOWLEDGMENTS

The authors would like to thank P.T. Antam UBPE Pongkor for the permission to publish this work. The researchers have carried out their research with support from both Bandung Institute of Technology and P.T. Antam UBPE Pongkor. Their support is gratefully acknowledged.

REFERENCES

- Al-Muqdad, S.W., Abo, R., Khattab, M.O. and Abdulhussein, F.M., 2020. Groundwater flow-modeling and sensitivity analysis in a hyper arid region. *Water*, 12 (8), p.21-31.
- Barker, J.A., 1988. A generalized radial flow model for hydraulic tests in fractured rock. *Water Resources Research*, 24 (10), p.1796-1804. DOI: 10.1029/WR024i010p01796
- Bense, V.F., Gleeson, T., Loveless, S.E., Bour, O., and Scibek, J., 2013. Fault zone hydrogeology. *Earth-Science Reviews*, 127, p.171-192. DOI:10.1016/j.earscirev.2013.09.008
- Cahyadi, T. A., Iskandar, I., Notosiswoyo, S., and Widodo, L. E., 2015. Studi Literatur Pendugaan Nilai Konduktivitas Hidraulik dengan Menggunakan Data Uji Hidraulik Lapangan dan Data Logging Geoteknik. Seminar Nasional Kebumihan X - FTM - UPN "Veteran" Yogyakarta, 498-504.
- Castro, M.C. and Goblet, P., 2003. Calibration of regional groundwater flow models: Working toward a better understanding of site-specific systems. *Water Resources Research*, 39 (6). DOI: 10.1029/2002WR001653
- Chowdhury, F., Gong, J., Rau, G.C. and Timms, W.A., 2022. Multifactor analysis of specific storage estimates and implications for tran-

- sient groundwater modelling. *Hydrogeology Journal*, 30 (7), p.2183-2204. DOI: 10.1007/s10040-022-02535-z
- Iskandar, I., Wibowo, A., Casanova, B. and Noto-siswoyo, S., 2014. A 3D Model of Hydraulic Conductivity Distribution of Fractured Rocks Using Packer Test Result and Geotechnical Log. *International Symposium on Earth Science and Technology, University of Kyushu, Japan*. DOI: 10.13140/2.1.2534.3046
- Ku, C.Y., Hsu, S.M., Chiou, L.B. and Lin, G.F., 2009. An empirical model for estimating hydraulic conductivity of highly disturbed clastic sedimentary rocks in Taiwan. *Engineering Geology*, 109 (3-4), p.213-223. DOI: 10.1016/j.enggeo.2009.08.008
- LAPI ITB, 2021. Project Report (Unpublished).
- Milesi, J.P., Marcoux, E., Sitorus, T., Simandjuntak, M., Leroy, J. and Bailly, L., 1999. Pongkor (West Java, Indonesia): a Pliocene supergene-enriched epithermal Au-Ag-(Mn) eposit. *Mineralium Deposita*, 34, p.131-149. DOI:10.1007/s001260050191
- M. Foster, L. and M. Maxwell, R., 2019. Sensitivity analysis of hydraulic conductivity and Manning's n parameters lead to new method to scale effective hydraulic conductivity across model resolutions. *Hydrological Processes*, 33 (3), p.332-349. DOI: 10.1002/hyp.13327
- P.T. Antam UBPE Pongkor, 2020. Studi Kelayakan Operasional (Unpublished).
- Surinaidu, L., Gurunadha Rao, V.V.S., Srinivasa, R., and Srinu, S.N., 2014. *Hydrogeological and groundwater modeling studies to estimate the groundwater inflows into the coal mines at different mine development stages using MODFLOW*, Andhra Pradesh, India. DOI:10.1016/j.wri.2014.10.002
- Zhang, C., Ma, Y., Zhang, C., and Liu, H., 2023. Sensitivity Analysis of the Physical Hydrological Model CASC2D-SED in Arid Area. *Polish Journal of Environmental Studies*, 32 (2). DOI: 10.15244/pjoes/157220
- Zhou, C.B., Chen, Y.F., Hu, R. and Yang, Z., 2023. Groundwater flow through fractured rocks and seepage control in geotechnical engineering: Theories and practices. *Journal of Rock Mechanics and Geotechnical Engineering*, 15 (1), p.1-36. DOI: 10.1016/j.jrmge.2022.10.001